Letter

Constraints on metastable superheavy dark matter coupled to sterile neutrinos with the Pierre Auger Observatory

A. Abdul Halim,[1] P. Abreu,[2] M. Aglietta,[3,4] I. Allekotte,[5] K. Almeida Cheminant,[6] A. Almela,[7,8] R. Aloisio,[9,10] J. Alvarez-Muñiz,[11] J. Ammerman Yebra,[11] G. A. Anastasi,[12,13] L. Anchordoqui,[14] B. Andrada,[7] S. Andringa,[2] L. Apollonio,[15,16] C. Aramo,[17] P. R. Araújo Ferreira,[18] E. Arnone,[19,4] J. C. Arteaga Velázquez,[20] P. Assis,[2] G. Avila,[21] E. Avocone,[22,10] A. Bakalova,[23] F. Barbato,[9,10] A. Bartz Mocellin,[24] J. A. Bellido,[1,25] C. Berat,[26] M. E. Bertaina,[19,4] G. Bhatta,[6] M. Bianciotto,[19,4] P. L. Biermann,[27] V. Binet,[28] K. Bismark,[29,7] T. Bister,[30,31] J. Biteau,[32,33] J. Blazek,[23] C. Bleve,[26] J. Blümer,[34] M. Boháčová,[23] D. Boncioli,[22,10] C. Bonifazi,[35,36] L. Bonneau Arbeletche,[37] N. Borodai,[6] J. Brack,[38] P. G. Brichetto Orchera,[7] F. L. Briechle,[18] A. Bueno,[39] S. Buitink,[40] M. Buscemi,[13,41] M. Büsken,[29,7] A. Bwembya,[30,31] K. S. Caballero-Mora,[42] S. Cabana-Freire,[11] L. Caccianiga,[15,16] F. Campuzano,[43] R. Caruso,[12,13] A. Castellina,[3,4] F. Catalani,[44] G. Cataldi,[45] L. Cazon,[11] M. Cerda,[46] A. Cermenati,[9,10] J. A. Chinellato,[37] J. Chudoba,[23] L. Chytka,[47] R. W. Clay,[1] A. C. Cobos Cerutti,[43] R. Colalillo,[48,17] M. R. Coluccia,[45] R. Conceição,[2] A. Condorelli,[32] G. Consolati,[16,49] M. Conte,[50,45] F. Convenga,[22,10] D. Correia dos Santos,[51] P. J. Costa,[2] C. E. Covault,[52] M. Cristinziani,[53] C. S. Cruz Sanchez,[54] S. Dasso,[55,56] K. Daumiller,[34] B. R. Dawson,[1] R. M. de Almeida,[51] J. de Jesús,[7,34] S. J. de Jong,[30,31] J. R. T. de Mello Neto,[36,57] I. De Mitri,[9,10] J. de Oliveira,[58] D. de Oliveira Franco,[45] F. de Palma,[50,45] V. de Souza,[59] B. P. de Souza de Errico,[36] E. De Vito,[50,45] A. Del Popolo,[12,13] O. Deligny,[60] N. Denner,[23] L. Deval,[34,7] A. di Matteo,[4] M. Dobre,[61] C. Dobrigkeit,[37] J. C. D'Olivo,[62] L. M. Domingues Mendes,[2,63] Q. Dorosti,[53] J. C. dos Anjos,[63] R. C. dos Anjos,[64] J. Ebr,[23] F. Ellwanger,[34] M. Emam,[30,31] R. Engel,[29,34] I. Epicoco,[50,45] M. Erdmann,[18] A. Etchegoyen,[7,8] C. Evoli,[9,10] H. Falcke,[30,65,31] G. Farrar,[66] A. C. Fauth,[37] N. Fazzini,[67] F. Feldbusch,[68] F. Fenu,[34,69] A. Fernandes,[2] B. Fick,[70] J. M. Figueira,[7] A. Filipčič,[71,72] T. Fitoussi,[34] B. Flaggs,[73] T. Fodran,[30] T. Fujii,[74,75] A. Fuster,[7,8] C. Galea,[30] C. Galelli,[15,16] B. García,[43] C. Gaudu,[76] H. Gemmeke,[68] F. Gesualdi,[7,34] A. Gherghel-Lascu,[61] P. L. Ghia,[60] U. Giaccari,[45] J. Glombitza,[18,77] F. Gobbi,[46] F. Gollan,[7] G. Golup,[5] M. Gómez Berisso,[5] P. F. Gómez Vitale,[21] J. P. Gongora,[21] J. M. González,[5] N. González,[7] D. Góra,[6] A. Gorgi,[3,4] M. Gottowik,[11] T. D. Grubb,[1] F. Guarino,[48,17] G. P. Guedes,[78] E. Guido,[53] L. Gülzow,[34] S. Hahn,[29] P. Hamal,[23] M. R. Hampel,[7] P. Hansen,[54] D. Harari,[5] V. M. Harvey,[1] A. Haungs,[34] T. Hebbeker,[18] C. Hojvat,[67] J. R. Hörandel,[30,31] P. Horvath,[47] M. Hrabovský,[47] T. Huege,[34,40] A. Insolia,[12,13] P. G. Isar,[79] P. Janecek,[23] V. Jilek,[23] J. A. Johnsen,[24] J. Jurysek,[23] K.-H. Kampert,[76] B. Keilhauer,[34] A. Khakurdikar,[30] V. V. Kizakke Covilakam,[7,34] H. O. Klages,[34] M. Kleifges,[68] F. Knapp,[29] J. Köhler,[34] N. Kunka,[68] B. L. Lago,[80] N. Langner,[18] M. A. Leigui de Oliveira,[81] Y. Lema-Capeans,[11] A. Letessier-Selvon,[82] I. Lhenry-Yvon,[60] L. Lopes,[2] L. Lu,[83] Q. Luce,[29] J. P. Lundquist,[72] A. Machado Payeras,[37] M. Majercakova,[23] D. Mandat,[23] B. C. Manning,[1] P. Mantsch,[67] F. M. Mariani,[15,16] A. G. Mariazzi,[54] I. C. Mariş,[84] G. Marsella,[41,13] D. Martello,[50,45] S. Martinelli,[34,7] O. Martínez Bravo,[85] M. A. Martins,[11] H.-J. Mathes,[34] J. Matthews,[86] G. Matthiae,[87,88] E. Mayotte,[24,76] S. Mayotte,[24] P. O. Mazur,[67] G. Medina-Tanco,[62] J. Meinert,[76] D. Melo,[7] A. Menshikov,[68] C. Merx,[34] S. Michal,[23] M. I. Micheletti,[28] L. Miramonti,[15,16] S. Mollerach,[5] F. Montanet,[26] L. Morejon,[76] C. Morello,[3,4] K. Mulrey,[30,31] R. Mussa,[4] W. M. Namasaka,[76] S. Negi,[23] L. Nellen,[62] K. Nguyen,[70] G. Nicora,[89] M. Niechciol,[53] D. Nitz,[70] D. Nosek,[90] V. Novotny,[90] L. Nožka,[47] A. Nucita,[50,45] L. A. Núñez,[91] C. Oliveira,[59] M. Palatka,[23] J. Pallotta,[89] S. Panja,[23] G. Parente,[11] T. Paulsen,[76] J. Pawlowsky,[76] M. Pech,[23] J. Pękala,[6] R. Pelayo,[92] L. A. S. Pereira,[93] E. E. Pereira Martins,[29,7] J. Perez Armand,[94] C. Pérez Bertolli,[7,34] L. Perrone,[50,45] S. Petrera,[9,10] C. Petrucci,[22,10] T. Pierog,[34] M. Pimenta,[2] M. Platino,[7] B. Pont,[30] M. Pothast,[31,30] M. Pourmohammad Shahvar,[41,13] P. Privitera,[74] M. Prouza,[23] S. Querchfeld,[76] J. Rautenberg,[76] D. Ravignani,[7] J. V. Reginatto Akim,[37] M. Reininghaus,[29] J. Ridky,[23] F. Riehn,[11] M. Risse,[53] V. Rizi,[22,10] W. Rodrigues de Carvalho,[30] E. Rodriguez,[7,34] J. Rodriguez Rojo,[21] M. J. Roncoroni,[7] S. Rossoni,[95] M. Roth,[34] E. Roulet,[5] A. C. Rovero,[55] P. Ruehl,[53] A. Saftoiu,[61] M. Saharan,[30] F. Salamida,[22,10] H. Salazar,[85] G. Salina,[88] J. D. Sanabria Gomez,[91] F. Sánchez,[7] E. M. Santos,[94] E. Santos,[23] F. Sarazin,[24] R. Sarmento,[2] R. Sato,[21] P. Savina,[83] C. M. Schäfer,[29] V. Scherini,[50,45] H. Schieler,[34] M. Schimassek,[60] M. Schimp,[76] D. Schmidt,[34] O. Scholten,[40,96] H. Schoorlemmer,[30,31] P. Schovánek,[23] F. G. Schröder,[73,34] J. Schulte,[18] T. Schulz,[34] S. J. Sciutto,[54] M. Scornavacche,[7,34] A. Sedoski,[7] A. Segreto,[97,13] S. Sehgal,[76] S. U. Shivashankara,[72] G. Sigl,[95] G. Silli,[7] O. Sima,[61,98] K. Simkova,[40] F. Simon,[68] R. Smau,[61] R. Šmída,[74] P. Sommers,[99] J. F. Soriano,[14] R. Squartini,[46] M. Stadelmaier,[16,15,34] S. Stanič,[72] J. Stasielak,[6] P. Stassi,[26] S. Strähnz,[29] M. Straub,[18] T. Suomijärvi,[32] A. D. Supanitsky,[7] Z. Svozilikova,[23] Z. Szadkowski,[100] F. Tairli,[1] A. Tapia,[101] C. Taricco,[19,4] C. Timmermans,[31,30] O. Tkachenko,[34] P. Tobiska,[23] C. J. Todero Peixoto,[44] B. Tomé,[2] Z. Torrès,[26] A. Travaini,[46] P. Travnicek,[23] C. Trimarelli,[22,10] M. Tueros,[54] M. Unger,[34] L. Vaclavek,[47] M. Vacula,[47] J. F. Valdés Galicia,[62] L. Valore,[48,17] E. Varela,[85] A. Vásquez-Ramírez,[91] D. Veberič,[34] C. Ventura,[57] I. D. Vergara Quispe,[54] V. Verzi,[88] J. Vicha,[23] J. Vink,[102]

S. Vorobiov,[72] C. Watanabe,[36] A. A. Watson,[103] A. Weindl,[34] L. Wiencke,[24] H. Wilczyński,[6] D. Wittkowski,[76] B. Wundheiler,[7] B. Yue,[76] A. Yushkov,[23] O. Zapparrata,[84] E. Zas,[11] D. Zavrtanik,[72,71] and M. Zavrtanik[71,72]

(The Pierre Auger Collaboration)[*]

[1]*University of Adelaide, Adelaide, S.A., Australia*
[2]*Laboratório de Instrumentação e Física Experimental de Partículas—LIP and Instituto Superior Técnico—IST, Universidade de Lisboa—UL, Lisbon, Portugal*
[3]*Osservatorio Astrofisico di Torino (INAF), Torino, Italy*
[4]*INFN, Sezione di Torino, Torino, Italy*
[5]*Centro Atómico Bariloche and Instituto Balseiro (CNEA-UNCuyo-CONICET), San Carlos de Bariloche, Argentina*
[6]*Institute of Nuclear Physics PAN, Krakow, Poland*
[7]*Instituto de Tecnologías en Detección y Astropartículas (CNEA, CONICET, UNSAM), Buenos Aires, Argentina*
[8]*Universidad Tecnológica Nacional—Facultad Regional Buenos Aires, Buenos Aires, Argentina*
[9]*Gran Sasso Science Institute, L'Aquila, Italy*
[10]*INFN Laboratori Nazionali del Gran Sasso, Assergi, L'Aquila, Italy*
[11]*Instituto Galego de Física de Altas Enerxías (IGFAE), Universidade de Santiago de Compostela, Santiago de Compostela, Spain*
[12]*Università di Catania, Dipartimento di Fisica e Astronomia "Ettore Majorana", Catania, Italy*
[13]*INFN, Sezione di Catania, Catania, Italy*
[14]*Department of Physics and Astronomy, Lehman College, City University of New York, Bronx, New York, USA*
[15]*Università di Milano, Dipartimento di Fisica, Milan, Italy*
[16]*INFN, Sezione di Milano, Milan, Italy*
[17]*INFN, Sezione di Napoli, Naples, Italy*
[18]*RWTH Aachen University, III. Physikalisches Institut A, Aachen, Germany*
[19]*Università Torino, Dipartimento di Fisica, Torino, Italy*
[20]*Universidad Michoacana de San Nicolás de Hidalgo, Morelia, Michoacán, Mexico*
[21]*Observatorio Pierre Auger and Comisión Nacional de Energía Atómica, Malargüe, Argentina*
[22]*Università dell'Aquila, Dipartimento di Scienze Fisiche e Chimiche, L'Aquila, Italy*
[23]*Institute of Physics of the Czech Academy of Sciences, Prague, Czech Republic*
[24]*Colorado School of Mines, Golden, Colorado, USA*
[25]*Universidad Nacional de San Agustin de Arequipa, Facultad de Ciencias Naturales y Formales, Arequipa, Peru*
[26]*Univ. Grenoble Alpes, CNRS, Grenoble Institute of Engineering Univ. Grenoble Alpes, LPSC-IN2P3, 38000 Grenoble, France*
[27]*Max-Planck-Institut für Radioastronomie, Bonn, Germany*
[28]*Instituto de Física de Rosario (IFIR)—CONICET/U.N.R. and Facultad de Ciencias Bioquímicas y Farmacéuticas U.N.R., Rosario, Argentina*
[29]*Karlsruhe Institute of Technology (KIT), Institute for Experimental Particle Physics, Karlsruhe, Germany*
[30]*IMAPP, Radboud University Nijmegen, Nijmegen, The Netherlands*
[31]*Nationaal Instituut voor Kernfysica en Hoge Energie Fysica (NIKHEF), Science Park, Amsterdam, The Netherlands*
[32]*Université Paris-Saclay, CNRS/IN2P3, IJCLab, Orsay, France*
[33]*Institut universitaire de France (IUF), France*
[34]*Karlsruhe Institute of Technology (KIT), Institute for Astroparticle Physics, Karlsruhe, Germany*
[35]*International Center of Advanced Studies and Instituto de Ciencias Físicas, ECyT-UNSAM and CONICET, Campus Miguelete—San Martín, Buenos Aires, Argentina*
[36]*Universidade Federal do Rio de Janeiro, Instituto de Física, Rio de Janeiro, Brazil*
[37]*Universidade Estadual de Campinas (UNICAMP), IFGW, Campinas, São Paulo, Brazil*
[38]*Colorado State University, Fort Collins, Colorado, USA*
[39]*Universidad de Granada and C.A.F.P.E., Granada, Spain*
[40]*Vrije Universiteit Brussels, Brussels, Belgium*
[41]*Università di Palermo, Dipartimento di Fisica e Chimica "E. Segrè", Palermo, Italy*
[42]*Universidad Autónoma de Chiapas, Tuxtla Gutiérrez, Chiapas, Mexico*

[43]*Instituto de Tecnologías en Detección y Astropartículas (CNEA, CONICET, UNSAM), and Universidad Tecnológica Nacional—Facultad Regional Mendoza (CONICET/CNEA), Mendoza, Argentina*
[44]*Universidade de São Paulo, Escola de Engenharia de Lorena, Lorena, São Paulo, Brazil*
[45]*INFN, Sezione di Lecce, Lecce, Italy*
[46]*Observatorio Pierre Auger, Malargüe, Argentina*
[47]*Palacky University, Olomouc, Czech Republic*
[48]*Università di Napoli "Federico II", Dipartimento di Fisica "Ettore Pancini", Naples, Italy*
[49]*Politecnico di Milano, Dipartimento di Scienze e Tecnologie Aerospaziali, Milan, Italy*
[50]*Università del Salento, Dipartimento di Matematica e Fisica "E. De Giorgi", Lecce, Italy*
[51]*Universidade Federal Fluminense, EEIMVR, Volta Redonda, Rio de Janeiro, Brazil*
[52]*Case Western Reserve University, Cleveland, Ohio, USA*
[53]*Universität Siegen, Department Physik—Experimentelle Teilchenphysik, Siegen, Germany*
[54]*IFLP, Universidad Nacional de La Plata and CONICET, La Plata, Argentina*
[55]*Instituto de Astronomía y Física del Espacio (IAFE, CONICET-UBA), Buenos Aires, Argentina*
[56]*Departamento de Física and Departamento de Ciencias de la Atmósfera y los Océanos, FCEyN, Universidad de Buenos Aires and CONICET, Buenos Aires, Argentina*
[57]*Universidade Federal do Rio de Janeiro (UFRJ), Observatório do Valongo, Rio de Janeiro, Brazil*
[58]*Instituto Federal de Educação, Ciência e Tecnologia do Rio de Janeiro (IFRJ), Brazil*
[59]*Universidade de São Paulo, Instituto de Física de São Carlos, São Carlos, Brazil*
[60]*CNRS/IN2P3, IJCLab, Université Paris-Saclay, Orsay, France*
[61]*"Horia Hulubei" National Institute for Physics and Nuclear Engineering, Bucharest-Magurele, Romania*
[62]*Universidad Nacional Autónoma de México, Mexico City, Mexico*
[63]*Centro Brasileiro de Pesquisas Fisicas, Rio de Janeiro, Rio de Janeiro, Brazil*
[64]*Universidade Federal do Paraná, Setor Palotina, Palotina, Brazil*
[65]*Stichting Astronomisch Onderzoek in Nederland (ASTRON), Dwingeloo, The Netherlands*
[66]*New York University, New York, New York, USA*
[67]*Fermi National Accelerator Laboratory, Fermilab, Batavia, Illinois, USA*
[68]*Karlsruhe Institute of Technology (KIT), Institut für Prozessdatenverarbeitung und Elektronik, Karlsruhe, Germany*
[69]*now at Agenzia Spaziale Italiana (ASI). Via del Politecnico 00133, Rome, Italy*
[70]*Michigan Technological University, Houghton, Michigan, USA*
[71]*Experimental Particle Physics Department, J. Stefan Institute, Ljubljana, Slovenia*
[72]*Center for Astrophysics and Cosmology (CAC), University of Nova Gorica, Nova Gorica, Slovenia*
[73]*University of Delaware, Department of Physics and Astronomy, Bartol Research Institute, Newark, Delaware, USA*
[74]*University of Chicago, Enrico Fermi Institute, Chicago, Illinois, USA*
[75]*now at Graduate School of Science, Osaka Metropolitan University, Osaka, Japan*
[76]*Bergische Universität Wuppertal, Department of Physics, Wuppertal, Germany*
[77]*ECAP, Erlangen, Germany*
[78]*Universidade Estadual de Feira de Santana, Feira de Santana, Brazil*
[79]*Institute of Space Science, Bucharest-Magurele, Romania*
[80]*Centro Federal de Educação Tecnológica Celso Suckow da Fonseca, Petropolis, Brazil*
[81]*Universidade Federal do ABC, Santo André, São Paulo, Brazil*
[82]*Laboratoire de Physique Nucléaire et de Hautes Energies (LPNHE), Sorbonne Université, Université de Paris, CNRS-IN2P3, Paris, France*
[83]*University of Wisconsin-Madison, Department of Physics and WIPAC, Madison, Wisconsin, USA*
[84]*Université Libre de Bruxelles (ULB), Brussels, Belgium*
[85]*Benemérita Universidad Autónoma de Puebla, Puebla, Mexico*
[86]*Louisiana State University, Baton Rouge, Louisiana, USA*
[87]*Università di Roma "Tor Vergata", Dipartimento di Fisica, Rome, Italy*
[88]*INFN, Sezione di Roma "Tor Vergata", Rome, Italy*
[89]*Laboratorio Atmósfera—Departamento de Investigaciones en Láseres y sus Aplicaciones—UNIDEF (CITEDEF-CONICET), Argentina*
[90]*Charles University, Faculty of Mathematics and Physics, Institute of Particle and Nuclear Physics, Prague, Czech Republic*
[91]*Universidad Industrial de Santander, Bucaramanga, Colombia*
[92]*Unidad Profesional Interdisciplinaria en Ingeniería y Tecnologías Avanzadas del Instituto Politécnico Nacional (UPIITA-IPN), Mexico City, Mexico*

[93]*Universidade Federal de Campina Grande, Centro de Ciencias e Tecnologia, Campina Grande, Brazil*
[94]*Universidade de São Paulo, Instituto de Física, São Paulo, Brazil*
[95]*Universität Hamburg, II. Institut für Theoretische Physik, Hamburg, Germany*
[96]*also at Kapteyn Institute, University of Groningen, Groningen, The Netherlands*
[97]*Istituto di Astrofisica Spaziale e Fisica Cosmica di Palermo (INAF), Palermo, Italy*
[98]*also at University of Bucharest, Physics Department, Bucharest, Romania*
[99]*Pennsylvania State University, University Park, Pennsylvania, USA*
[100]*University of Łódź, Faculty of High-Energy Astrophysics, Łódź, Poland*
[101]*Universidad de Medellín, Medellín, Colombia*
[102]*Universiteit van Amsterdam, Faculty of Science, Amsterdam, The Netherlands*
[103]*School of Physics and Astronomy, University of Leeds, Leeds, United Kingdom*

(Received 13 November 2023; accepted 13 March 2024; published 8 April 2024)

Dark matter particles could be superheavy, provided their lifetime is much longer than the age of the Universe. Using the sensitivity of the Pierre Auger Observatory to ultrahigh energy neutrinos and photons, we constrain a specific extension of the Standard Model of particle physics that meets the lifetime requirement for a superheavy particle by coupling it to a sector of ultralight sterile neutrinos. Our results show that, for a typical dark coupling constant of 0.1, the mixing angle θ_m between active and sterile neutrinos must satisfy, roughly, $\theta_m \lesssim 1.5 \times 10^{-6} (M_X/10^9\ \mathrm{GeV})^{-2}$ for a mass M_X of the dark-matter particle between 10^8 GeV and 10^{11} GeV.

DOI: 10.1103/PhysRevD.109.L081101

Introduction. Despite its countless successes, the Standard Model (SM) of particle physics is known to be incomplete. Missing elements include, among others, dark matter (DM) and neutrino masses. A minimal extension to the SM is to add right-handed neutrinos inert to SM interactions ("sterile" neutrinos) that mix with left-handed ones active under weak interactions ("active" neutrinos) via the Brout-Englert-Higgs mechanism. Sub-eV mass eigenvalues result from mixing angles made sufficiently small by highly enough massive sterile neutrinos (seesaw mechanism [1,2]). Other extensions may use additional sterile neutrinos, as their number is in general largely underconstrained. This is the case of the extension presented in [3], considered in this study as a beyond-standard-model (BSM) benchmark. In this model, which includes DM and neutrino masses, a second sterile neutrino is assumed to render metastable a superheavy particle referred to as X with mass M_X and lifetime τ_X, the decay products of which can leave unique signatures in the data of the Pierre Auger Observatory [4].

A superheavy particle that is metastable attracts particular attention if it is to be a viable DM candidate. The constraints imposed on τ_X are indeed demanding; $\tau_X \gtrsim 10^{22}$ yr, see e.g., [5–11] for recent estimates in various channels. Compliance with these constraints indeed calls for adjusting a reduced coupling constant α_X down to a tiny level and, simultaneously, the multiplicity of the final state to a large value [12,13]. This is in general challenging for theoretical constructions, unless the decay rules are based on nonperturbative effects [14,15]. In the BSM benchmark [3], however, the lifetime does not resort to such a fine tuning. The DM particle X interacts only with sub-eV and superheavy (10^{12}–10^{14} GeV) sterile neutrinos, of masses m_N and M_N respectively, via Yukawa couplings y_m and y_M. In the mass-eigenstate basis, neutrinos are then quasiactive or quasisterile, depending on the mixture of active and sterile neutrinos governed by a small mixing angle $\theta_m \simeq \sqrt{2} y_m v/m_\nu$, with v the electroweak scale and m_ν the mass of the known neutrinos. To leading order in y_m, quasiactive neutrinos are produced from quasisterile ones subsequent to the decay of X. Consequently, the coupling y_m controls the dominant decay channels and allows for trading a factor $(M_X/M_\mathrm{P})^2$ (with M_P the Planck mass) for a $(m_\nu \theta_m/v)^2$ one in the decay width of X. This trading enables the reduction of the width by a factor $\sim 10^{-25}\theta_m^2$ for a benchmark value $M_X = 10^9$ GeV, leading to the required lifetimes well beyond the age of the Universe.

Ultrahigh energy (UHE) neutrinos and photons are expected to emerge from the cascade of the X decay. In this paper, we use the sensitivity of the Pierre Auger Observatory to such neutrinos and photons to impose constraints on the active-sterile neutrino mixing angle θ_m for DM masses $M_X \gtrsim 10^8$ GeV. After recalling the main features of the observatory that enable the detection of neutrinos and photons, we present the main decay channels of the X particle. We then calculate the number of neutrinos and photons expected to be observed at the observatory as a

*spokespersons@auger.org; http://www.auger.org

function of θ_m and M_X. Their nonobservation allows us to constrain θ_m for $M_X \gtrsim 10^8$ GeV. In a last section, we comment on the complementary bounds obtained on M_X from DM abundance and on θ_m from cosmological observations.

Pierre auger observatory. The Pierre Auger Observatory is the largest ground-based observatory that exploits extensive air showers to study UHE cosmic rays [4]. Several detection techniques are combined. A surface of $3,000\ \mathrm{km}^2$ is covered with a ground array of particle detectors separated by 1,500 m surrounded by fluorescence detectors spread over four sites. This baseline configuration is complemented with low-energy enhancements; a first nested array of $24\ \mathrm{km}^2$ with particle detectors separated by 750 m and overlooked by three additional fluorescence telescopes with an elevated field of view, and a second one of $1.14\ \mathrm{km}^2$ with detectors separated by 433 m, some of them on top of buried scintillation modules used to measure the number of high-energy muons. The fluorescence detectors provide, during moonless nights, direct observation of the longitudinal shower profile, which allows for the measurement of the energy and the primary-mass sensitive depth of the shower maximum, $X_{\max}$. On the other hand, the ground-level and underground detectors sample the shower particles with a permanent duty cycle. Although showers are observed at a fixed slice in depth with this technique, their longitudinal development is embedded in the signals detected.

Neutrinos of all flavors can be distinguished from nuclei through showers developing deeply in the atmosphere at large zenith angles (down-going detection mode) [16], while tau neutrinos can undergo charged-current interactions and produce a τ lepton in the crust of the Earth that eventually decays in the atmosphere, inducing an upward-going shower (Earth-skimming detection mode) [17]. In both cases, neutrinos can be identified at the Observatory with signals in the ground-level particle detectors that are spread over time, by contrast to narrow ones expected from the much more abundant nuclei-induced showers at large zenith angles [18–20]. Photon-induced showers have also distinct salient features [21,22]. Their first interactions are of electromagnetic nature, and the transfer of energy to the hadron/muon channel is reduced with respect to the bulk of hadron-induced showers. This results in a lower number of secondary muons. Additionally, as the development of photon showers is delayed by the typically small multiplicity of electromagnetic interactions, their $X_{\max}$ is deeper in the atmosphere than for showers initiated by hadrons.

Based on these characteristics, a number of analyses have been designed to make the most of the sensitivity of the different detectors of the Observatory to neutrinos above $\simeq 10^8$ GeV [23] and to photons above 5×10^7 GeV [24–27]. The nonobservation of point sources and diffuse fluxes allowed the derivation of upper bounds that constrain various models very effectively. In the following, we draw constraints on the BSM benchmark [3] from these nonobservations.

The bsm benchmark. In the BSM benchmark [3], the DM candidate is a pseudoscalar particle X coupled to the sterile neutrinos sector alone. The interaction can be represented diagrammatically as

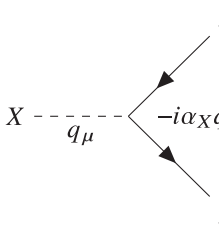

(1)

with q the four-momentum of X, and γ the Dirac matrices. Sterile neutrinos, which are right-handed, are denoted as N. Two types of Majorana sterile neutrinos are actually introduced. The first type, N_M, corresponds to the right-handed neutrino of the seesaw mechanism, with a superheavy mass M_N. The second type, N_m, with mass m_N, is necessary to allow the X particle to decay in an electroweak channel. In the basis of interaction eigenstates, the couplings between sterile neutrinos, active neutrinos and SM Higgs isospinor scalar fields through Yukawa parameters y_m and y_M give rise, after symmetry breakdown, to Dirac masses $m^{\mathrm{D}}_{N_m} = y_m v/\sqrt{2}$ and $m^{\mathrm{D}}_{N_M} = y_M v/\sqrt{2}$. Assuming the hierarchy $m_N < m^{\mathrm{D}}_{N_M} \ll M_N$, the three mass eigenstates associated to the eigenvalues (m_1, m_2, m_3) are well-approximated by the following mixing between ν_{L} (active neutrinos), N_M and N_m (and their conjugate partners with superscripts 'c':

$$\nu_1 \simeq (N_m + {N_m}^{\mathrm{c}}) + \theta_m(\nu_{\mathrm{L}} + {\nu_{\mathrm{L}}}^{\mathrm{c}}), \tag{2}$$

$$\nu_2 \simeq (\nu_{\mathrm{L}} + {\nu_{\mathrm{L}}}^{\mathrm{c}}) - \theta_m(N_m + {N_m}^{\mathrm{c}}), \tag{3}$$

$$\nu_3 \simeq N_M, \tag{4}$$

with the mixing angle θ_m, assumed to be $\ll 1$, defined as $\theta_m \simeq y_m v/\sqrt{2}(m_1 + m_2)$. For small mixings, the first (second) mass eigenstate ν_1 (ν_2) is almost the light sterile (active) neutrino with a small admixture of the active (sterile) one, and that the third mass eigenstate ν_3 is almost the superheavy sterile neutrino. Note that to avoid complications that would be irrelevant to the question of DM, the flavor couplings in the active neutrino sector are considered diagonal in this study. The three mass eigenvalues read as

$$m_1 \simeq m_N, \tag{5}$$

$$m_2 \simeq y_m^2 v^2/2M_N, \tag{6}$$

$$m_3 \simeq M_N. \tag{7}$$

The third eigenstate ν_3 appears to decouple from the two other states. While the superheavy particle N_M is essential to provide the mass to the active neutrino through a mixing angle $\theta_M = y_M v/2M_N$ identical to that of the standard seesaw mechanism [1,2], we shall ignore ν_3 hereafter. From the constraints on SM neutrino masses $\sum m_\nu \leq 0.12$ eV inferred from cosmological observations [28], we use hereafter $m_2 \simeq 0.04$ eV as a benchmark. As for m_1, following [3], we use $m_1 = 10^{-4}$ eV to fix the ideas; we shall see below that as long as $m_1 \ll m_2$, results are not sensitive to the specific choice. That $m_1 \ll m_2$ is required for the lifetime of X to be much larger than the age of the universe.

To leading order in θ_m, the interaction described by Eq. (1) gives rise, in the basis of mass eigenstates, to the two-body decay $X \to \nu_1\nu_1$. However, in the relevant parameter space such that $m_1 \ll m_2 \ll m_e \ll m_Z \ll M_X$, the total width Γ^X is dominated by three-body channels stemming from the diagram depicted in Eq. (1) and the interaction between active/sterile neutrinos and the Higgs isodoublet with Yukawa coupling $y_m \simeq \sqrt{2}\theta_m m_2/v$. The channel $X \to h\nu_1\nu_2$, diagrammatically represented as

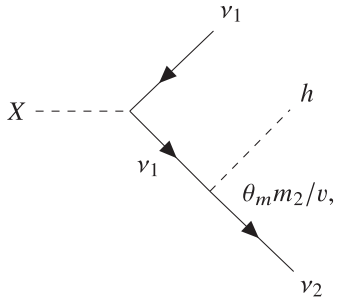

(8)

gives the most important contribution to the width [3],

$$\Gamma^X_{h\nu_1\nu_2} = \frac{\alpha_X^2\theta_m^2}{192\pi^3}\left(\frac{M_X}{M_{\rm P}}\right)^2\left(\frac{m_2}{v}\right)^2 M_X. \tag{9}$$

Due to the structure of the interaction depicted in Eq. (1), a factor $(M_X/M_{\rm P})^2$ expected from dimensional arguments [12] is traded for a factor $(m_2/v)^2$.

Although subdominant, there are two other three-body decay channels of interest, namely $X \to Z\nu_1\nu_2$ and $X \to W\nu_1 e$ with respective widths,

$$\Gamma^X_{Z\nu_1\nu_2} = \frac{\alpha_X^2 g^2\theta_m^2}{798\pi^3\cos^2\theta_{\rm W}}\left(\frac{M_X}{M_{\rm P}}\right)^2\left(\frac{m_2}{m_Z}\right)^2 M_X, \tag{10}$$

$$\Gamma^X_{W\nu_1 e} = \frac{\alpha_X^2 g^2\theta_m^2}{768\pi^3}\left(\frac{M_X}{M_{\rm P}}\right)^2\left(\frac{m_1}{m_W}\right)^2 M_X, \tag{11}$$

with g the weak-isospin gauge constant and $\theta_{\rm W}$ the Weinberg angle. These two widths share the same structure as $\Gamma^X_{h\nu_1\nu_2}$ modulo smaller numerical factors.

Ultrahigh energy neutrinos and photons. UHE neutrinos and photons are expected as byproducts of the decay of any particle with a mass much larger than the electroweak scale. Ultimately, they result from splitting-particle effects due to soft or collinear (real) radiative corrections enhanced by large logarithmic factors at high scale. The probability that a particle a at a scale μ_a fragments to produce a particle b at a scale μ_b carrying a fraction x of the initial energy is described by a fragmentation function (FF) $D_a^b(x;\mu_a,\mu_b)$. The FFs are evolved starting from measurements at the electroweak scale up to the energy scale M_X. In the QCD sector, the evolution is governed by DGLAP equations to account for the splitting function that describes the emission of parton k by parton j. The resulting prompt spectra of photons and neutrinos have been derived in [29] and in several subsequent studies. Similarly, electroweak cascading can be described by evolution equations valid for a spontaneously broken theory [30]. Seminal works of [29,31,32] in the QCD sector and of [33] in the electroweak one have provided the calculation of the FFs to derive the prompt flux of high-energy secondaries from the decay of a particle at high scale. We use hereafter the up-to-date HDMSpectra tool [34] to calculate the energy spectra of UHE neutrinos and photons from the decay of the X particle in the $X \to h\nu_1\nu_2$, $X \to Z\nu_1\nu_2$ and $X \to W\nu_1 e$ channels.

The number of neutrinos $n_\nu(E)$ expected to be observed above an energy threshold E results from the integration over the sky of the directional exposure $\mathcal{E}_\nu(E,\mathbf{n})$ of the observatory and of the flux of neutrinos emitted isotropically in proportion to the DM density accumulated in galaxy halos [35],

$$n_\nu(E) = \int\!\!\int_{\geq E} {\rm d}\mathbf{n}\,{\rm d}E'\frac{\mathcal{E}_\nu(E',\mathbf{n})}{4\pi M_X}\left[\frac{{\rm d}\Gamma_\nu(E')}{{\rm d}E'}\int {\rm d}s\,\rho(\mathbf{x}_\odot + s\mathbf{n}) + \Omega_X\rho_{\rm c}\int {\rm d}z\frac{e^{-S_\nu(E',z)}}{(1+z)H(z)}\frac{{\rm d}\Gamma_\nu(E^\star)}{{\rm d}E'}\bigg|_{E^\star=(1+z)E'}\right]. \tag{12}$$

The first contribution is from the Milky Way halo, in which the DM energy density is parameterized by a profile function $\rho(\mathbf{x})$. $\mathbf{x}_\odot$ is the position of the Solar system in the Galaxy, s is the distance from $\mathbf{x}_\odot$ to the emission point, and $\mathbf{n} \equiv \mathbf{n}(\ell, b)$ is a unit vector on the sphere pointing to the longitude ℓ and latitude b, in Galactic coordinates. There are uncertainties in the determination of the Galactic-halo profile. We use here the traditional Navarro-Frenk-White profile as a reference [36],

$$\rho_{\rm DM}(R) = \frac{\rho_s}{(R/R_s)(1+R/R_s)^2}, \tag{13}$$

where R is the distance to the Galactic center, $R_s = 24$ kpc, and ρ_s is fixed by the DM density in the solar neighborhood, namely $\rho_\odot = 0.44\ {\rm GeV\,cm^{-3}}$ [37]. To quantify the

systematics stemming from the uncertainties on this profile, we repeat the analysis using other ones [38–40]. The second contribution in Eq. (12), which is obtained by integration over redshift z and which amounts to about 10% of the first one, is from all other galaxies. ρ_c is the critical energy density, Ω_X is the DM abundance, $S_\nu(E,z)$ is the neutrino opacity of the Universe as calculated in [41], and the Hubble rate $H(z)$ depends on that observed today, H_0, and on the total matter abundance, Ω_m, through $H(z)=H_0\sqrt{\Omega_m(1+z)^3+(1-\Omega_m)}$. In both contributions, the particle X decays into a (SM) daughter particle I whose FF leads to neutrinos. Thus, the differential decay width into neutrinos, $d\Gamma_\nu/dE$, results from the convolution of the differential decay width of X to I with the FF of I into neutrinos. For a single flavor, it reads as

$$\frac{d\Gamma_\nu}{dE}=\frac{2}{\Gamma^X}\sum_I\int_x^1\frac{dy}{y}\frac{d\Gamma_I^X(y)}{dy}D_I^\nu\left(\frac{x}{y},\frac{M_X}{2},0\right), \quad (14)$$

with $x=2E_\nu/M_X$. In the $h\nu_1\nu_2$ channel, the differential decay width reads as

$$\frac{d\Gamma_\nu^{X\to h\nu_1\nu_2}(y)}{dy}=3\Gamma^X_{h\nu_1\nu_2}y^2, \quad (15)$$

for neutrino final states, while it reads as

$$\frac{d\Gamma_h^{X\to h\nu_1\nu_2}(y)}{dy}=6\Gamma^X_{h\nu_1\nu_2}y(1-y), \quad (16)$$

for Higgs final states [3]. Similar expressions hold in the cases of the $Z\nu_1\nu_2$ and $W\nu_1 e$ channels, with the corresponding decay widths. Finally, the differential widths entering into Eq. (14) account for all detectable flavors for the $\nu_{2\alpha}$ species, where an explicit flavor index α is reintroduced. In the down-going detection mode, the three flavors contribute explicitly as

$$\begin{aligned}\frac{d\Gamma_{\nu_{2,\mathrm{all}}}}{dE}=&\frac{2}{\Gamma^X}\int_x^1\frac{dy}{y}\left[\sum_\alpha\left(\frac{d\Gamma_h^{X\to h}(y)}{dy}D_h^{\nu_{2\alpha}}\left(\frac{x}{y}\right)\right.\right.\\&+\frac{d\Gamma_Z^{X\to Z}(y)}{dy}D_Z^{\nu_{2\alpha}}\left(\frac{x}{y}\right)+2\frac{d\Gamma_W^{X\to W}(y)}{dy}D_W^{\nu_{2\alpha}}\left(\frac{x}{y}\right)\Big)\\&+\sum_{\alpha,\beta}\left(\frac{d\Gamma_\nu^{X\to h}(y)}{dy}D_{\nu_{2\beta}}^{\nu_{2\alpha}}\left(\frac{x}{y}\right)+\frac{d\Gamma_\nu^{X\to Z}(y)}{dy}D_{\nu_{2\beta}}^{\nu_{2\alpha}}\left(\frac{x}{y}\right)\right)\\&\left.+\sum_\alpha 2\frac{d\Gamma_\nu^{X\to W}(y)}{dy}D_e^{\nu_{2\alpha}}\left(\frac{x}{y}\right)\right], \quad (17)\end{aligned}$$

with flavor indices α and β. Additionally, the nonzero probability for neutrinos in the final state for "no-splitting" leads to an extra contribution,

$$D_{\nu_{2\alpha}}^{\nu_{2\alpha}}\left(\frac{x}{y},\frac{M_X}{2},0\right)\simeq\xi\delta\left(\frac{x}{y}-1\right), \quad (18)$$

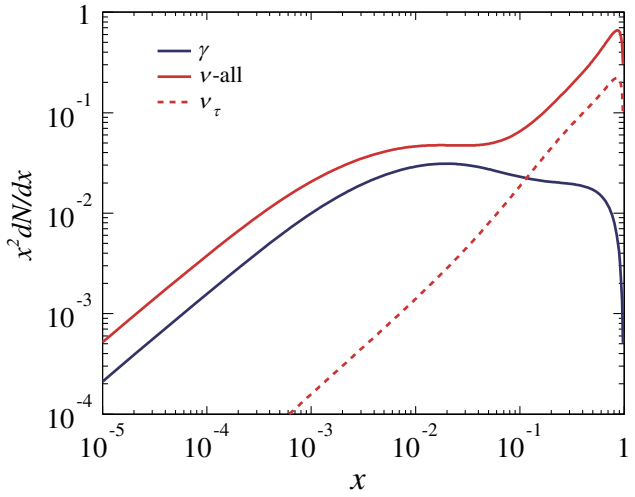

FIG. 1. Energy spectrum of neutrinos and photons from the decay of the pseudoscalar particle X within the BSM benchmark [3] ($M_X=10^{10}$ GeV).

with $\xi=0.13$. The contribution to the Earth-skimming detection mode is obtained similarly, considering only the τ flavor. Besides, the differential decay width into photons is also calculated following the same procedure, with proper FFs. Note that the expected photon fluxes to be compared to the flux limits are almost entirely determined by the contribution of the Milky Way halo (due to their attenuation over inter-galactic scales). The resulting energy spectra are shown in Fig. 1 for $M_X=10^{10}$ GeV. The high-energy enhancements are shaped by the nonzero probabilities for splitting a few times only at high scales.

Constraints in the planes (τ_X,M_X) and (θ_m,M_X). Constraints in the planes (τ_X,M_X) and (θ_m,M_X) can be derived from the nonobservation of neutrinos at the Observatory. First, 90% C.L. lower limits on the lifetime τ_X are obtained by setting, for a specific value of M_X, $n_\nu(E)$, or $n_\gamma(E)$ to the 90% C.L. upper-limit numbers corresponding to the number of background-event candidates in the absence of signal [42,43]. More details about the upper-limit numbers for each specific analysis searching for neutrinos or photons are provided in the supplemental material [44]. Subsequently, a scan in M_X is carried out. It leads to a curve in the plane (τ_X,M_X) that pertains to the energy threshold E considered. By repeating the procedure for several thresholds, a set of curves is obtained, reflecting the sensitivity of a specific energy threshold to some range of mass M_X. The union of the excluded regions finally provides the constraints in the (τ_X,M_X) plane. Results are shown in Fig. 2 (top panel); lifetimes within the cross-hatched region are excluded. The region in full red pertains to a particular value of a Yukawa coupling $\lambda_{N_m}=10^{-5}$, the meaning of which will be explained below. To illustrate the contribution from each secondary at our disposal, we show as the dotted the contribution to the

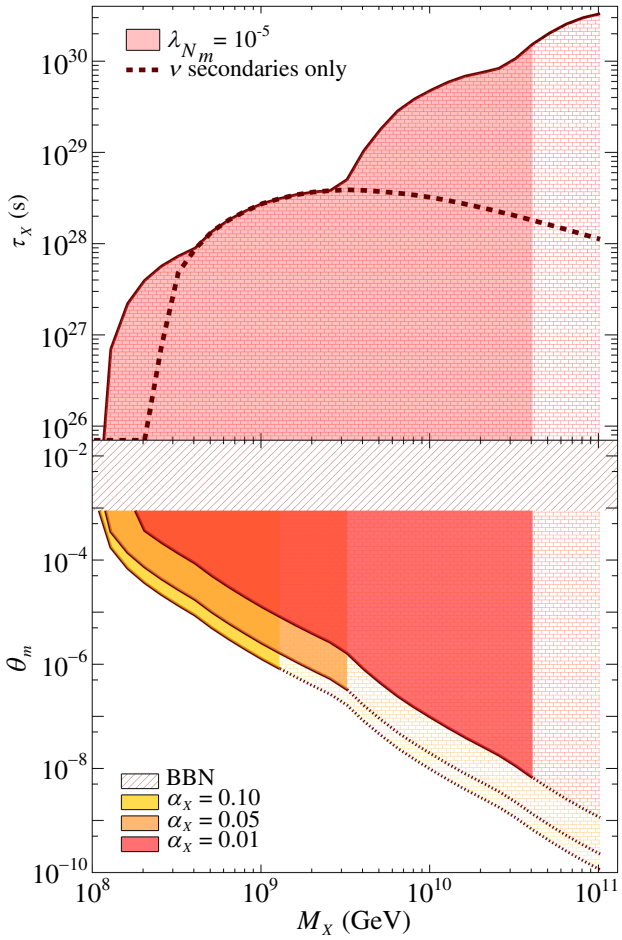

FIG. 2. *Top*: Constraints on τ_X as a function of M_X for a value of the couplings of sterile neutrinos with the inflationary sector $\lambda_{N_m} = 10^{-5}$. The dotted line illustrates the constraints stemming from neutrino secondaries alone. *Bottom*: Constraints on θ_m as a function of M_X for three different values of the coupling constant α_X, still for $\lambda_{N_m} = 10^{-5}$. The hatched-red region $\theta_m \geq 9 \times 10^{-4}$ is excluded from the constraint on $\Delta N_{\rm eff}$ (see text).

constraints stemming from neutrinos alone; an analysis of the IceCube exposure dedicated to the benchmark-scenario decay channels would likely provide better sensitivity for exploring masses $M_X \lesssim 10^{8.5}$ GeV. The lower limit on τ_X is then transformed into an upper limit on θ_m using the expressions of the total width of the particle X. Results are shown in the bottom panel for separate values of α_X; color-coded regions pertain to $\lambda_{N_m} = 10^{-5}$ while their extension (in cross-hatched) would require smaller values of λ_{N_m}. Systematic uncertainties on θ_m constraints amount overall to $\simeq \pm 15\%$; they are dominated by those on the neutrino exposure [23]. The restricted ranges of M_X for different α_X values come from the requirements not to overclose the Universe with DM, while the exclusion hatched band comes from not altering the expansion history of the Universe with the presence of ultralight species such as sterile neutrinos N_m. We now briefly explain how these constraints are obtained.

In addition to its couplings to the DM sector and to the SM one through the Higgs isodoublet, the sterile neutrino N_m is also coupled to an inflationary sector in the BSM benchmark [3]. This coupling, governed by a unique Yukawa parameter λ_{N_m} for every ν_1 neutrinos, yields to a "radiative" production of X via a diagram similar to that depicted in Eq. (8) (substituting X by the inflaton Φ in the initial state, and h and ν_2 by X and ν_1 in the final states). Such a mechanism leads to a direct production of DM during the reheating period that can be sufficient, in general, to match the right amount of DM observed today [45]. In the BSM benchmark [3], values for λ_{N_m} are then required to range preferentially around 10^{-5}. To infer the DM density n_X produced mainly during the reheating epoch, we also consider the minimal setup of gravitational production of X particles through the annihilation of SM (inflaton) particles as in [46] (as in [47]). In these conditions, X particles can be produced as long as the collision rate of particles is larger than the expansion rate H and/or as long as the inflaton field oscillates. By contrast, n_X is prohibitively low to allow any thermal equilibrium for DM. The collision term in the Boltzmann equation is then approximated as a source term only. Overall, the Boltzmann equation reads as

$$\frac{{\rm d}n_X(t)}{{\rm d}t} + 3H(t)n_X(t) = \sum_i \bar{n}_i^2(t)\gamma_i + \bar{n}_\phi(t)\Gamma_{X\nu_1\nu_1}. \qquad (19)$$

Here, the sum on the right hand side represents the contributions from the SM and inflationary sectors. Using, on the one hand, the evolution of the SM matter and inflaton densities derived in [48] and [47], respectively, and, on the other hand, the SM + SM $\to X + X$ and $\Phi + \Phi \to X + X$ reaction rates γ_i derived in [49] and [47], respectively, the present-day relic abundance of DM can then be related, using Eq. (19) in the same way as in [15], to the mass M_X, the Hubble rate at the end of inflation $H_{\rm inf}$, and the reheating efficiency ε quantifying the duration of the reheating period ($\varepsilon = 1$ for an instantaneous reheating) [46]. As a result, viable couples of values for $(H_{\rm inf}, M_X)$ scale as $H_{\rm inf} \propto M_X^2$ up to a maximum value for M_X, which depend on ε and α_X. This scaling is a consequence of the domination of the radiative-production process over the gravitational one as long as the allowed values of $H_{\rm inf}$ are too small for a given M_X value to generate significant particle production by gravitational interactions. For larger masses, the contribution from gravitational interactions added to the radiative production of X leads to an overproduction of DM that overcloses the universe, and there is thus no longer solution. This explains why the color-coded regions extend up to some maximum values of M_X in Fig. 2, for a benchmark value of $\lambda_{N_m} = 10^{-5}$. To the right of the regions shown in cross-hatched, λ_{N_m} would need to be smaller.

Another constraint on θ_m stems from the upper bound on the departure from 3 of the effective number of neutrino degrees of freedom $N_{\rm eff}$, $\Delta N_{\rm eff} = N_{\rm eff} - 3$, inferred from

cosmological observations. From Friedmann equation, the Hubble parameter is governed by the energy-density content, which, during the radiation-dominated epoch, receives contributions from all relativistic species such as photons, active neutrinos and possible sterile ones. A significant value of $\Delta N_{\rm eff}$ would thus change the dynamics of the expansion during the radiation era and thus impact on the cosmological microwave background measurements as well as on the big bang nucleosynthesis. Therefore, the 95% confidence-level current limits on $\Delta N_{\rm eff} < 0.3$ [50] provide constraints on the temperature T_{ν_1} of ν_1 neutrinos;

$$\Delta N_{\rm eff} = \frac{3}{2}\left(\frac{T_{\nu_1}}{T_{\nu_2}}\right)^4 < 0.3. \tag{20}$$

This relationship is valid at any time before the radiation era started, in particular at the time each neutrino species decoupled from the thermal bath when the expansion rate became larger than the interaction rate R_{ν_i} of the species ν_i. Given that the ratio H/R_{ν_i} scales as $(T/T_{\star\nu_i})^3$ [51] (denoting as $T_{\star\nu_i}$ the decoupling temperature of ν_i), and given that the neutral-current interaction rate of the ν_1 species is that of ν_2 but reduced by θ_m^2, the relation $T_{\star\nu_1} = \theta_m^{-2/3} T_{\star\nu_2}$ holds. As soon as T dropped below $T_{\star\nu_1}$, the temperature of the freely expanding ν_1 species fell as $T_{\nu_1} = (a_{\star 1}/a) T_{\star\nu_1}$ (with $a_{\star 1}$ the scale factor at the time of the decoupling of the ν_1 species). At temperatures $T < T_{\star\nu_1}$, other particles that are still in thermal equilibrium, such as electrons and positrons, annihilate once T becomes smaller than their mass and thus heat the rest of the relativistic species (photons) relative to the neutrinos. Entropy conservation in this "freeze-out" then gives rise to the relationship,

$$\left(\frac{T_{\nu_1}(T_{\star\nu_2})}{T_{\star\nu_2}}\right)^3 = \frac{\mathcal{N}_{\star 2}}{\mathcal{N}_{\star 1}}, \tag{21}$$

with $\mathcal{N}_{\star i}$ the number of degrees of freedom at $a = a_{\star i}$. Combining Eq. (20) and Eq. (21) with $\mathcal{N}_{\star 2} = 43/4$ (accounting for two photon-polarization states, three species of neutrinos and three of antineutrinos, and electrons and positrons each with two spin states) and $T_{\star\nu_2} = 2$ MeV [51], we obtain that $\mathcal{N}_{\star 1} \gtrsim 35.95$ and thus, using [52] to convert $\mathcal{N}$ into a temperature, the following bound on θ_m:

$$\theta_m \leq \left(\frac{T_{\star\nu_2}}{T_{\star\nu_1}}\right)^{3/2} \simeq \left(\frac{2\ \text{MeV}}{215\ \text{MeV}}\right)^{3/2} \simeq 9 \times 10^{-4}. \tag{22}$$

This bound is shown as the cross-hatched band in Fig. 2.[1]

[1]Once translated in terms of effective sterile neutrino mass and $\Delta N_{\rm eff}$ (see e.g., [53]), the constraints on neutrino mass-squared difference between eigenstates and on mixing angles between mass and flavour eigenstates inferred from neutrino-oscillation experiments are within the dark red band.

Conclusion. In conclusion, we have shown that the data of the Pierre Auger Observatory provide stringent constraints on the angle θ_m mixing sub-eV sterile and active neutrinos in the context of an extension to the SM that couples the sterile neutrinos to a superheavy DM candidate [3]. For a typical dark coupling constant of 0.1, the mixing angle θ_m must satisfy, roughly, $\theta_m \lesssim 1.5 \times 10^{-6} (M_X/10^9\ \text{GeV})^{-2}$ for a mass M_X of the dark-matter particle between 10^8 GeV and 10^{11} GeV. Future sensitivity to the effective number of neutrino degrees of freedom $\Delta N_{\rm eff}$ from cosmological observations will be complementary, as they will probe θ_m below 10^{-3} independent of the mass M_X. In particular, a value of $\Delta N_{\rm eff}$ departing significantly from 3 would call for sterile neutrinos and would fix the range of the mixing angle θ_m. Our constraints would then be decisive in determining whether the new physics thus revealed in the neutrino sector is intimately related to that of superheavy DM.

Acknowledgments. The successful installation, commissioning, and operation of the Pierre Auger Observatory would not have been possible without the strong commitment and effort from the technical and administrative staff in Malargüe. We are very grateful to the following agencies and organizations for financial support: Argentina—Comisión Nacional de Energía Atómica; Agencia Nacional de Promoción Científica y Tecnológica (ANPCyT); Consejo Nacional de Investigaciones Científicas y Técnicas (CONICET); Gobierno de la Provincia de Mendoza; Municipalidad de Malargüe; NDM Holdings and Valle Las Leñas; in gratitude for their continuing cooperation over land access; Australia—the Australian Research Council; Belgium—Fonds de la Recherche Scientifique (FNRS); Research Foundation Flanders (FWO); Brazil—Conselho Nacional de Desenvolvimento Científico e Tecnológico (CNPq); Financiadora de Estudos e Projetos (FINEP); Fundação de Amparo à Pesquisa do Estado de Rio de Janeiro (FAPERJ); São Paulo Research Foundation (FAPESP) Grants No. 2019/10151-2, No. 2010/07359-6, and No. 1999/05404-3; Ministério da Ciência, Tecnologia, Inovações e Comunicações (MCTIC); Czech Republic Grants No. MSMT CR LTT18004, No. LM2015038, No. LM2018102, No. CZ.02.1.01/0.0/0.0/16_013/0001402, No. CZ.02.1.01/0.0/0.0/18_046/0016010, and No. CZ.02.1.01/0.0/0.0/17_049/0008422; France—Centre de Calcul IN2P3/CNRS; Centre National de la Recherche Scientifique (CNRS); Conseil Régional Ile-de-France; Département Physique Nucléaire et Corpusculaire (PNC-IN2P3/CNRS); Département Sciences de l'Univers (SDU-INSU/CNRS); Institut Lagrange de Paris (ILP) Grant No. LABEX ANR-10-LABX-63 within the Investissements d'Avenir Programme Grant No. ANR-11-IDEX-0004-02; Germany—Bundesministerium für Bildung und Forschung (BMBF); Deutsche Forschungsgemeinschaft (DFG); Finanzministerium Baden-Württemberg; Helmholtz

Alliance for Astroparticle Physics (HAP); Helmholtz-Gemeinschaft Deutscher Forschungszentren (HGF); Ministerium für Innovation, Wissenschaft und Forschung des Landes Nordrhein-Westfalen; Ministerium für Wissenschaft, Forschung und Kunst des Landes Baden-Württemberg; Italy—Istituto Nazionale di Fisica Nucleare (INFN); Istituto Nazionale di Astrofisica (INAF); Ministero dell'Istruzione, dell'Universitá e della Ricerca (MIUR); CETEMPS Center of Excellence; Ministero degli Affari Esteri (MAE); México—Consejo Nacional de Ciencia y Tecnología (CONACYT) No. 167733; Universidad Nacional Autónoma de México (UNAM); PAPIIT DGAPA-UNAM; The Netherlands—Ministry of Education, Culture and Science; Netherlands Organisation for Scientific Research (NWO); Dutch national e-infrastructure with the support of SURF Cooperative; Poland—Ministry of Education and Science, Grant No. DIR/WK/2018/11; National Science Centre, Grants No. 2016/22/M/ST9/00198, No. 2016/23/B/ST9/01635, and No. 2020/39/B/ST9/01398; Portugal—Portuguese national funds and FEDER funds within Programa Operacional Factores de Competitividade through Fundação para a Ciência e a Tecnologia (COMPETE); Romania—Ministry of Research, Innovation and Digitization, CNCS/CCCDI—UEFISCDI, Projects No. PN19150201/16N/2019, No. PN1906010, TE128, and No. PED289, within PNCDI III; Slovenia—Slovenian Research Agency, Grants No. P1-0031, No. P1-0385, No. NI0-0033, and No. N1-0111; Spain—Ministerio de Economía, Industria y Competitividad (FPA2017-85114-P and PID2019–104676GB-C32), Xunta de Galicia (ED431C 2017/07), Junta de Andalucía (SOMM17/6104/UGR, P18-FR-4314) Feder Funds, RENATA Red Nacional Temática de Astropartículas (FPA2015-68783-REDT) and María de Maeztu Unit of Excellence (MDM-2016-0692); USA—Department of Energy, Contracts No. DE-AC02-07CH11359, No. DE-FR02-04ER41300, No. DE-FG02-99ER41107, and No. DE-SC0011689; National Science Foundation, Grant No. 0450696; The Grainger Foundation; Marie Curie-IRSES/EPLANET; European Particle Physics Latin American Network; and UNESCO. We acknowledge for this work the support of the Institut Pascal at Université Paris-Saclay during the Paris-Saclay Astroparticle Symposium 2022, with the support of the P2IO Laboratory of Excellence (program "Investissements d'avenir" ANR-11-IDEX-0003-01 Paris-Saclay and ANR-10-LABX-0038), the P2I axis of the Graduate School of Physics of Université Paris-Saclay, as well as IJCLab, CEA, APPEC, IAS, OSUPS, and the IN2P3 master projet UCMN. Finally, we thank S. Cléry, Y. Mambrini and M. Pierre for numerous discussions about the BSM benchmark studied in this work.

[1] M. Gell-Mann, P. Ramond, and R. Slansky, Conf. Proc. C **790927**, 315 (1979).
[2] T. Yanagida, Prog. Theor. Phys. **64**, 1103 (1980).
[3] E. Dudas, L. Heurtier, Y. Mambrini, K. A. Olive, and M. Pierre, Phys. Rev. D **101**, 115029 (2020).
[4] A. Aab *et al.* (Pierre Auger Collaboration), Nucl. Instrum. Methods Phys. Res., Sect. A **798**, 172 (2015).
[5] M. Kachelriess, O. E. Kalashev, and M. Y. Kuznetsov, Phys. Rev. D **98**, 083016 (2018).
[6] E. Alcantara, L. A. Anchordoqui, and J. F. Soriano, Phys. Rev. D **99**, 103016 (2019).
[7] K. Ishiwata, O. Macias, S. Ando, and M. Arimoto, J. Cosmol. Astropart. Phys. 01 (2019) 003.
[8] C. Guépin, R. Aloisio, L. A. Anchordoqui, A. Cummings, J. F. Krizmanic, A. V. Olinto, M. H. Reno, and T. M. Venters, Phys. Rev. D **104**, 083002 (2021).
[9] C. Bérat, C. Bleve, O. Deligny, F. Montanet, P. Savina, and Z. Torrès, Astrophys. J. **929**, 55 (2022).
[10] R. Abbasi *et al.* (IceCube Collaboration), J. Cosmol. Astropart. Phys. 10 (2023) 003.
[11] S. Das, K. Murase, and T. Fujii, Phys. Rev. D **107**, 103013 (2023).
[12] H. J. de Vega and N. G. Sanchez, Phys. Rev. D **67**, 125019 (2003).
[13] P. Abreu *et al.* (Pierre Auger Collaboration), Phys. Rev. D **107**, 042002 (2023).
[14] V. A. Kuzmin and V. A. Rubakov, Phys. At. Nucl. **61**, 1028 (1998).
[15] P. Abreu *et al.* (Pierre Auger Collaboration), Phys. Rev. Lett. **130**, 061001 (2023).
[16] K. S. Capelle, J. W. Cronin, G. Parente, and E. Zas, Astropart. Phys. **8**, 321 (1998).
[17] X. Bertou, P. Billoir, O. Deligny, C. Lachaud, and A. Letessier-Selvon, Astropart. Phys. **17**, 183 (2002).
[18] J. Abraham *et al.* (Pierre Auger Collaboration), Phys. Rev. Lett. **100**, 211101 (2008).
[19] P. Abreu *et al.* (Pierre Auger Collaboration), Phys. Rev. D **84**, 122005 (2011); **84**, 029902(E) (2011).
[20] A. Aab *et al.* (Pierre Auger Collaboration), Phys. Rev. D **91**, 092008 (2015).
[21] P. Billoir, in *Physics and Astrophysics of UHECRs*, edited by M. Lemoine and G. Sigl (Springer, New York, 2000), pp. 27–44.
[22] M. Risse and P. Homola, Mod. Phys. Lett. A **22**, 749 (2007).
[23] A. Aab *et al.* (Pierre Auger Collaboration), J. Cosmol. Astropart. Phys. 10 (2019) 022.
[24] P. Abreu *et al.* (Pierre Auger Collaboration), Astrophys. J. **933**, 125 (2022).
[25] P. Savina *et al.* (Pierre Auger Collaboration), *Proc. Sci.*, ICRC2021 (2021) 373.
[26] P. Abreu *et al.* (Pierre Auger Collaboration), J. Cosmol. Astropart. Phys. 05 (2023) 021.

[27] N. Gonzalez *et al.* (Pierre Auger Collaboration), Proc. Sci. ICRC2023 (**2023**) 238.
[28] N. Aghanim *et al.* (Planck Collaboration), Astron. Astrophys. **641**, A6 (2020); **652**, C4(E) (2021).
[29] R. Aloisio, V. Berezinsky, and M. Kachelriess, Phys. Rev. D **69**, 094023 (2004).
[30] M. Ciafaloni, P. Ciafaloni, and D. Comelli, Phys. Rev. Lett. **88**, 102001 (2002).
[31] S. Sarkar and R. Toldra, Nucl. Phys. **B621**, 495 (2002).
[32] C. Barbot and M. Drees, Astropart. Phys. **20**, 5 (2003).
[33] V. Berezinsky, M. Kachelriess, and S. Ostapchenko, Phys. Rev. Lett. **89**, 171802 (2002).
[34] C. W. Bauer, N. L. Rodd, and B. R. Webber, J. High Energy Phys. 06 (2021) 121.
[35] R. Aloisio, S. Matarrese, and A. V. Olinto, J. Cosmol. Astropart. Phys. 08 (2015) 024.
[36] J. F. Navarro, C. S. Frenk, and S. D. M. White, Astrophys. J. **462**, 563 (1996).
[37] Y. Jiao, F. Hammer, H. Wang, J. Wang, P. Amram, L. Chemin, and Y. Yang, Astron. Astrophys. **678**, A208 (2023).
[38] J. Einasto, Tr. Astrofiz. Inst. Alma-Ata **5**, 87 (1965).
[39] A. Burkert, Astrophys. J. Lett. **447**, L25 (1995).
[40] B. Moore, S. Ghigna, F. Governato, G. Lake, T. R. Quinn, J. Stadel, and P. Tozzi, Astrophys. J. Lett. **524**, L19 (1999).
[41] P. Gondolo, G. Gelmini, and S. Sarkar, Nucl. Phys. **B392**, 111 (1993).
[42] G. J. Feldman and R. D. Cousins, Phys. Rev. D **57**, 3873 (1998).
[43] J. Conrad, O. Botner, A. Hallgren, and C. Perez de los Heros, Phys. Rev. D **67**, 012002 (2003).
[44] See Supplemental Material at http://link.aps.org/supplemental/10.1103/PhysRevD.109.L081101 for a description of the directional exposure of the Observatory to photons and neutrinos.
[45] K. Kaneta, Y. Mambrini, and K. A. Olive, Phys. Rev. D **99**, 063508 (2019).
[46] M. Garny, M. Sandora, and M. S. Sloth, Phys. Rev. Lett. **116**, 101302 (2016).
[47] Y. Mambrini and K. A. Olive, Phys. Rev. D **103**, 115009 (2021).
[48] D. J. H. Chung, E. W. Kolb, and A. Riotto, Phys. Rev. D **59**, 023501 (1998).
[49] M. Garny, A. Palessandro, M. Sandora, and M. S. Sloth, J. Cosmol. Astropart. Phys. 02 (2017) 027.
[50] N. Aghanim *et al.* (Planck Collaboration), Astron. Astrophys. **641**, A1 (2020).
[51] S. Weinberg, *Cosmology* (Oxford Press, Oxford, 2008).
[52] L. Husdal, Galaxies **4**, 78 (2016).
[53] S. Bridle, J. Elvin-Poole, J. Evans, S. Fernandez, P. Guzowski, and S. Soldner-Rembold, Phys. Lett. B **764**, 322 (2017).